Environmental Science
Water Research & Technology

PAPER

Cite this: *Environ. Sci.: Water Res. Technol.*, 2025, **11**, 1568

Insights into the degradation of carbamazepine using a continuous-flow non-thermal plasma: kinetics and comparison with UV-based systems

Samuel O. Babalola, Michael O. Daramola and Samuel A. Iwarere *

Received 17th December 2024,
Accepted 25th April 2025

DOI: 10.1039/d4ew01042f

rsc.li/es-water

The widespread presence of carbamazepine (CBZ) in the environment and its potential impacts on non-target organisms and ecosystem dynamics raise concerns globally. In this study the degradation of CBZ was studied using an atmospheric dielectric barrier discharge (DBD) reactor. The influence of different operating parameters such as the initial concentration of the pollutant, applied voltage, pH, and conductivity on the DBD performance was investigated based on CBZ degradation efficiency. At optimal conditions (10 mg L^{-1}, 6 kV, and 5 μS cm^{-1}), a 92% degradation efficiency for CBZ was achieved. The process was less effective in an acidic medium but enhanced in neutral and slightly alkaline conditions. This study also investigated the active role of reactive species like O_3, H_2O_2, ·OH, and $\cdot O_2^-$ produced during the treatment process. To evaluate the efficacy of the DBD system in real conditions, experiments were also performed in tap water and in final wastewater effluent within a 40 min treatment time. Lastly, the degradation efficiency of the DBD reactor, energy efficiency, and energy cost were compared with those of UV-only, UV/Fe^{2+}, UV/H_2O_2, and UV/H_2O_2/Fe^{2+} systems. For all the parameters investigated, the DBD plasma used in this work demonstrated superior performance to that of the UV-assisted systems, while the UV-only system gave the worst performance.

Water impact

Carbamazepine (CBZ) is considered to be a contaminant of emerging concern due to its persistence in various water sources. CBZ is also known to be an endocrine-disrupting contaminant that poses numerous threats to the health of living organisms that are subject to long-term exposure to it. It is noted that conventional wastewater treatment plants are ineffective in removing this contaminant; therefore, other means must be employed. This study provides a detailed insight into an emerging advanced oxidation technology, namely a non-thermal plasma, and a well-known ultraviolet light radiation method and investigates their ability to degrade CBZ in different water matrices such as deionised water, tap water and final wastewater effluent from a municipal wastewater treatment plant. Although common research of such nature explores synthetic water samples using deionised water, the studies into different water matrices are rare, and thus the scientific community is usually unsure if the same results obtained for deionised water are going to be obtained for real wastewater samples.

1. Introduction

Active pharmaceutical contaminants are continually introduced into surface and groundwater through anthropogenic activities, including discharges from wastewater treatment plants (WWTPs), run-off from agricultural fields, aquaculture facilities, and the application of biosolids or manure to soils.[1–3] Additional sources include effluents from pharmaceutical manufacturing sites, hospital waste streams, human excretion of parent compounds and metabolites, as well as the improper disposal of unused or expired medications into sewage systems. Among these contaminants, carbamazepine (CBZ) has garnered attention due to its extensive use and persistence in conventional and biological treatment systems.[4–6] CBZ is commonly prescribed for antiepileptic and mood-stabilizing medication, with an annual global consumption of about 1014 tons, and it has been ubiquitously detected in diverse water sources, including drinking water.[7–10] While the direct impact of CBZ on human health remains unclear, its pervasive presence in aquatic environments raises concerns regarding its potential effects on non-target organisms and ecosystem stability.

To mitigate the environmental burden of pharmaceutical pollutants, regulatory frameworks have been proposed in several developed countries to ensure the safe discharge of

Sustainable Energy and Environment Research Group (SEERG), Department of Chemical Engineering, Faculty of Engineering, Built Environment and Information Technology (EBIT), University of Pretoria, Hatfield, Pretoria 0002, South Africa. E-mail: samuel.iwarere@up.ac.za; Tel: +27 12 420 3092

pharmaceutical substances.[11,12] However, the development of such policies is complex, requiring a delicate balance between environmental protection, public health, and accessibility to essential medications. One proposed strategy for enhancing pharmaceutical removal in WWTPs is the integration of advanced oxidation processes (AOPs), which are highly effective in degrading persistent contaminants.[13] The intrinsic advantage of AOPs lies in their ability to produce active highly potent species like hydroxy radicals (·OH) which can potentially oxidize pollutants into less toxic by-products. Thus, coupling AOPs with existing WWTP setups will help create a sophisticated system that can remove a myriad of pollutants regardless of their specific properties or concentrations.

Several AOPs have been examined in the degradation of persistent pharmaceutical pollutants. In the case of CBZ, UV-assisted AOP systems like UV/H_2O_2, UV/H_2O_2/Fe^{2+} and UV/H_2O_2/Fe^{3+} have yielded 60.2%, 90.6%, and 74.3% degradation efficiencies, respectively, according to a study by Ali *et al.*[14] This study highlights the critical role of iron catalysts in facilitating the generation of ·OH radicals, which drive the degradation of CBZ. Meanwhile, CBZ itself was said to be highly resistant to a direct photolysis system as only 7.5% degradation was achieved. In another similar study by Zou *et al.*,[15] ferrous-activated sodium hypochlorite (NaOCl) was employed to degrade CBZ in a soil system, achieving 94.5% degradation within 4 h at an optimal Fe^{2+}/NaOCl (1 : 1) molar ratio. This study reaffirmed the importance of ·OH generation to CBZ degradation.

Beyond hydroxyl radicals, other reactive species also contribute to CBZ degradation. For instance, sulfate radicals ($SO_4^{-\bullet}$) have demonstrated strong oxidative potential. Wang and Zhou[16] achieved 89.4% CBZ degradation within 120 min using a combined ultrasound/persulfate system, highlighting the efficacy of $SO_4^{-\bullet}$ in CBZ oxidation. Similarly, Guo *et al.*[17] reported that $SO_4^{-\bullet}$ was superior to ·OH in CBZ degradation through radical quenching experiments. A hybrid AOP system combining hydrodynamic cavitation (HC) with UV/persulphate and composite ZnO/$ZnFe_2O_4$ catalysts was developed by Roy and Moholkar,[18] achieving 98.13% CBZ degradation in 60 min. Comparatively, HC alone resulted in only 7.7%, while HC/$Na_2S_2O_8$ achieved 65.73% degradation, demonstrating the synergistic benefits of dual-radical (·OH and $SO_4^{-\bullet}$) production. Photocatalysis has also been widely explored for CBZ degradation, leveraging solar irradiation and semiconductor materials to generate reactive species. Ding *et al.*[19] reported a photocatalytic oxidation of CBZ using Bi^{3+} self-doped $NaBiO_3$ nanosheets with a nearly complete degradation efficiency (99.8%) in 60 min. Other photocatalysts like TiO_2,[20] $ZnIn_2S_4$,[21] BiOCl and BiOCl/AgCl composite[22] have also demonstrated high degradation efficiencies. Ozone-based AOPs have been similarly effective in CBZ degradation. For example, Asghar *et al.*[23] achieved complete CBZ degradation using sulfur-doped graphene-enhanced ozonation. Yang *et al.*[24] used an electro-peroxone process, where *in situ* generation of O_3 and H_2O_2 resulted in 99.8% degradation efficiency and 97.6% mineralization within 15 min and 90 min, respectively. The advantage of these approaches lies in the synergistic interaction of O_3 with H_2O_2 and catalytic minerals, enhancing ·OH production for more efficient pollutant breakdown. Despite the demonstrated efficacy of these AOPs, several limitations persist, including poor light penetration, lamp fouling, high energy consumption, the production of toxic by-products, and challenges in catalyst activation and recovery.

In this study, a non-thermal plasma (NTP) system was investigated for the degradation of CBZ. NTP-based AOPs are gaining attention for their simplicity, effectiveness, energy efficiency, scalability, and additive-free operation. Unlike other AOPs that primarily generate a single type of reactive species, plasma discharges produce a complex mixture of UV radiation, O_3, ·OH and other radicals, H_2O_2, and shock waves, creating a synergistic degradation effect with minimal selectivity concerns and reduced toxic byproducts. Various NTP configurations have been explored in previous studies for CBZ degradation, including dielectric barrier discharge (DBD)[25] and corona discharge.[26] Gwanzura *et al.*[27] achieved about 93% degradation efficiency using a point-to-plane electrical discharge system operated in a batch mode. Rayaroth *et al.*[28] compared the performance of a DBD plasma system in deionized water and tap water to examine the effect of natural ions in real water. Yu *et al.*[29] demonstrated enhanced CBZ degradation using Fe^{2+}-assisted DBD plasma, reinforcing the role of iron ions in promoting ·OH radical formation. However, a key limitation of these studies is their low throughput. Some authors have also combined the plasma system with other AOPs. For example, in a recent study by Ahlawat *et al.*[30] a plasma-UV hybrid AOP gave >92% CBZ degradation efficiency in 15 min compared to a plasma-only setup, which yielded only about 20% degradation in the same time.

This study makes significant advancements in plasma-based water treatment by introducing atmospheric air-based continuous-flow DBD plasma, systematically analyzing the contribution of reactive species, and evaluating the effect of real water matrices. While previous studies relied on controlled gas compositions (*e.g.*, oxygen, argon), the use of natural atmospheric air aims to reduce the operational costs associated with plasma treatment. Considering that several studies have reported the efficacy of UV-based treatment, the last objective focused on the comparison of the DBD plasma with UV-based systems in terms of degradation performance, energy efficiency, and the energy cost of treatment.

2. Materials and methods

2.1. Materials

CBZ ($C_{15}H_{12}N_2O$) with >99% purity was purchased from Leapchem (China). Deionized water obtained from an Elga LabWater Chorus 1 device was used in preparing the working solutions used in this experiment. Tap water was collected from the University of Pretoria, South Campus at building 4,

while final wastewater effluent was collected from the Daspoort municipality in Pretoria. Isopropanol (IPA, C_3H_8O) was supplied by Radchem (PTY) Ltd (South Africa), and *p*-benzoquinone (BZQ, $C_6H_4O_2$), sodium pyruvate (SP, $C_3H_3NaO_3$), and uric acid (UA, $C_5H_4N_4O_3$) were purchased from Sigma-Aldrich (USA). Iron(II) sulphate heptahydrate ($FeSO_4{\cdot}7H_2O$) and hydrogen peroxide (H_2O_2, 30%) were obtained from Merck (Germany). The pH of solutions was adjusted with sodium hydroxide (NaOH) and sulphuric acid (H_2SO_4) obtained from Glassworld (South Africa). All chemicals were of analytical grade and were used without further purification.

a. DBD plasma experiments. The DBD plasma experimental setup is shown in Fig. 1. The major equipment used in this study consists of a high voltage (HV) AC power supply, a continuous-flow DBD reactor, a peristaltic pump, a digital oscilloscope, and a high-performance liquid chromatography (HPLC) system used in analyzing the treated solution samples. The important features of the reactor are provided in Table 1. The reactor consists of a hollow multi-pin stainless-steel rod positioned at the centre of a borosilicate glass tube with 35.4 mm inner diameter and 2.3 mm wall thickness. The stainless-steel rod serves as the HV electrode to which the AC power supply is connected, while a conductive copper tape was used as the ground electrode. Atmospheric air was used as the working gas in this experiment to generate discharges at the edge of the pins of the HV electrode. The contaminated water is pumped upwards from the storage tank through the hollow HV electrode, and it is dispersed evenly *via* a microjet placed at the top of the HV electrode in the glass tube. The falling water film then contacts the discharge produced at the multi-pins and gets collected back into the storage container. Recirculation of water was ensured by a peristaltic pump (Integra, China). The required AC voltage is generated by a custom-made AC voltage power supply fabricated by Jeenel Technologies Pty Ltd, South Africa. The applied voltage and discharge current of the plasma reactor were measured with a digital oscilloscope (Rigol DS1074Z Plus, 70 MHz). Although the use of a water falling film is not a new concept in plasma water treatment, what specifically distinguishes the system used in this study lies in the use of spikes at the edge of the inner electrode which significantly reduced the voltage required to create the discharge even for a gap of 5 mm between the electrode and inner glass tube compared to 4 mm for Kooshki *et al.*[31] and 4.5 mm in Kovačević *et al.*[32]

Table 1 Technical characteristics and operating conditions for the DBD plasma reactor

Reactor information	Value/description
Type of glass	Borosilicate tube
Length of glass tube	30 cm
HV electrode material	Stainless steel
Length of HV electrode	29 cm
Diameter of HV electrode	1.7 cm
Discharge length	6.9 mm
AC voltage applied	4–6 kV
AC frequency	20 kHz
Power drawn from the grid at 6 kV	125 W
Concentration of CBZ examined	10–30 mg L^{-1}
Treated volume	1 L
Water flow rate	500 mL min^{-1}

Scavenging experiments were set up using IPA, UA, BZQ, and SP to investigate the possible contributions of ·OH, O_3, $\cdot O_2^-$, and H_2O_2, respectively. The synthetic solutions containing each of these scavengers were prepared in deionized water at different concentrations. The DBD plasma degradation experiment was also performed in tap water and final wastewater effluent to examine the effect of water matrices on the degradation of CBZ. The key properties of the synthetic water, tap water, and final wastewater effluent are summarized in Table 2.

b. UV experiments. The setup for the UV-based experiments (UV only, UV/Fe^{2+}, UV/H_2O_2, and UV/Fe^{2+}/H_2O_2) is shown in Fig. 2. The degradation was performed in a photochemical reactor equipped with a 254 nm UV lamp (supplied by Lelesil Innovation Systems) and operated in a

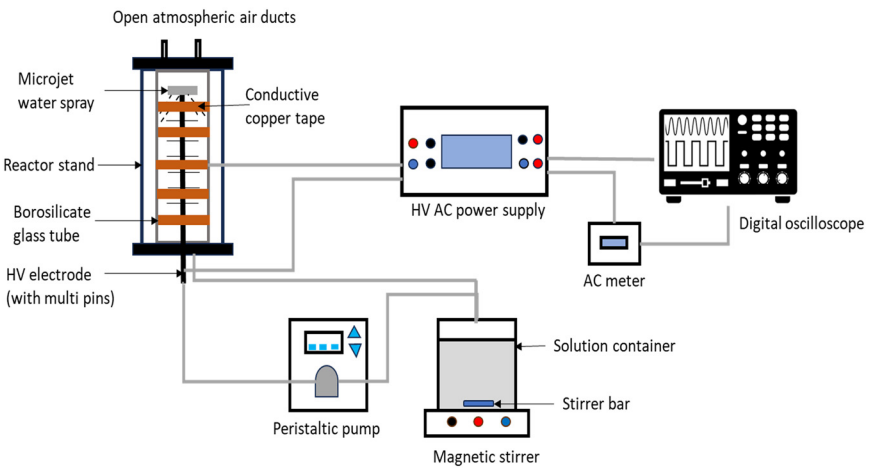

Fig. 1 Experimental setup for the dielectric barrier discharge plasma system.

batch mode.[33,34] The photoreactor used in this study is comprised of a 1 L volume quartz-jacketed tube hosting a 250 W high-pressure mercury vapour lamp (HPMVL; UV light lamp), a 4 L cooling tank, a magnetic stirrer, and a protective compartment. 500 mL CBZ solution was exposed to the UV treatment for 40 min, and the solution was stirred at 400 rpm. Samples of the treated solution were withdrawn using a syringe at 5 min intervals for analysis.

2.2. Analytical procedure

The residual CBZ concentrations in the aqueous solutions were monitored by an Alliance Waters 2695 HPLC system equipped with a Waters 2489 UV/vis detector (285 nm) and a 4.6 mm × 250 mm C18 5 μm column. The mobile phase consisted of methanol and deionized water (50 : 50, v/v) with a flow rate of 1 mL min^{-1} and 10 μL injection volume. The efficiencies for degradation of CBZ in the experiments were calculated using eqn (1):

$$\eta\,(\%) = \frac{C_i - C_t}{C_i}(100) \quad (1)$$

where η represents the degradation efficiency for CBZ (%), C_i represents the initial concentration of CBZ (mg L^{-1}) and C_t represents the concentration of CBZ at a particular treatment time (min) in the solution (mg L^{-1}). The degradation efficiency provides an insight into the performance of the technology used in degrading the pollutant. Also, the kinetic analysis of CBZ fitted a pseudo-first-order rate according to eqn (2):

$$\ln\left(\frac{C_i}{C_t}\right) = kt \quad (2)$$

where C_i and C_t have the same definitions as in eqn (1), k is the reaction rate constant (min^{-1}) and t is the treatment time (min).

The pH and conductivity measurements were performed using a HANNA multiparameter H198194 meter. The concentration of hydrogen peroxide (H_2O_2) and ozone (O_3) in the solution was determined by spectrophotometry using a Lovibond Spectrodirect water testing instrument (Tintometer Group, Germany) to investigate the yield of these species in the DBD plasma. An ion chromatography instrument (940 Professional IC Vario, Metrohm, Germany) was used in measuring the anions in the solution.

Table 2 Characteristics of deionized water, tap water, and final wastewater effluent

Parameters	Deionized water	Tap water	Final wastewater effluent
pH	5.7	7.53	7.3
Conductivity (μS cm^{-1})	5	270	544
Nitrates (NO_3^-, mg L^{-1})	—	12.2	15.2
Nitrites (NO_2^-, mg L^{-1})	—	0.1	1
Sulphate (SO_4^-, mg L^{-1})	—	23.3	57.5
Chloride (Cl^-, mg L^{-1})	—	20.8	52.7
Hydrogen carbonate (HCO_3^-, mg L^{-1})	—	99.6	150.5

3. Results and discussion

3.1. Investigation of the reactive species generated in the DBD plasma

A typical DBD at the gas–liquid interface can prompt diverse chemical reactions which eventually result in the production of a broad range of highly reactive chemical species such as free radicals (·OH, ·H, ·O, HO_2·), neutral molecules (O_3, H_2O_2) as well as other positive and negative ions. These species have different oxidizing potentials, and as mentioned earlier, they provide a combined effect in degrading organic pollutants in aqueous solutions. Also, the amount of the reactive species generated by a DBD plasma system and their effectiveness are affected by certain factors such as input energy, type of gas used and the flow rate, pH of the solution, and conductivity in some cases, amongst others.[35] Some of these are discussed in detail in subsequent sections.

$$H_2O_2 + h\nu \rightarrow \cdot OH + \cdot OH \quad (3)$$

$$H_2O_2 + \cdot OH \rightarrow HO_2\cdot + H_2O \quad (4)$$

$$HO_2\cdot + \cdot OH \rightarrow O_2 + H_2O \quad (5)$$

Among the generated reactive species, ·OH has been the most desired due to its strong oxidizing property (E° = 2.85 V) and non-selectivity toward pollutants. It reacts with most organic matters by hydrogen abstraction with saturated aliphatic hydrocarbons or by electrophilic addition with unsaturated hydrocarbons.[36] The recombination of ·OH produced in a gas–liquid plasma system generates H_2O_2 (E° = 1.77 V), which is another important species that facilitates the oxidation of organic pollutants.[37] The concentration of H_2O_2 can provide insight into the measure of ·OH available in the aqueous solution. This is because ·OH radicals have a short half-time while H_2O_2 is relatively stable. Therefore, to understand the mechanism and efficacy of the degradation of CBZ, the concentration of H_2O_2 was measured during CBZ (10 mg L^{-1}) degradation at an applied voltage of 6 kV and frequency of 20 kHz. According to Fig. 3, the concentration of H_2O_2 increased with time, reaching a peak of 6.7 mg L^{-1} in 30 min. Afterward, it decreased to 5.6 mg L^{-1} at the end of the treatment time. The decomposition of H_2O_2 after reaching its highest concentration can be explained by its reaction with the active species present in the discharge based on eqn (3)–(5), and also by the effect of an increase in the solution temperature (from 22 to 45 °C) as also reported by Kirkpatrick and Locke.[38]

$$*e^- + O_2 \rightarrow \cdot O + \cdot O + e^- \quad (6)$$

$$O_2 + \cdot O \rightarrow O_3 \quad (7)$$

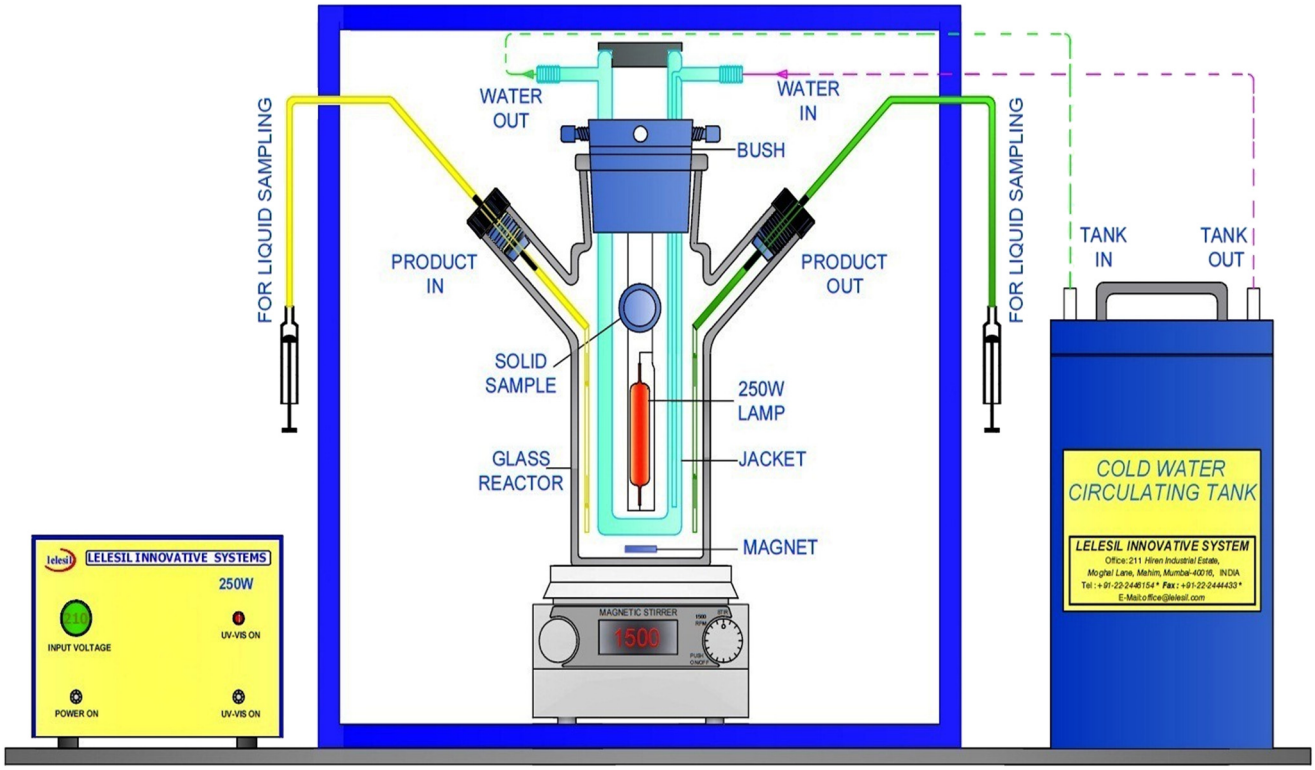

Fig. 2 Setup for the UV-based experiments.

$$O_3 + H_2O_2 \rightarrow \cdot OH + O_2 + HO_2^{\cdot} \quad (8)$$

$$O_3 + \cdot OH \rightarrow O_2 + HO_2^{\cdot} \quad (9)$$

$$O_3 + HO_2^{\cdot} \rightarrow \cdot OH + O_2 + \cdot O_2^{-} \quad (10)$$

Also, the presence of oxygen in the atmospheric air gas used induces a reaction between the highly energized electrons and oxygen, leading to the production of reactive oxygen species such as ozone (O_3) and $^{\cdot}O$, according to eqn (6) and (7). Meanwhile, O_3 (E^{o} = 2.07 V) is also a powerful oxidizing agent that can react effectively with organic pollutants through a series of reactions.[39] The concentration of O_3 produced in the DBD plasma system had a similar trend to that of H_2O_2, as shown in Fig. 3. The decline in concentration observed after 30 min could also be attributed to the temperature increase observed in the solution.[40] Also, O_3 can react with H_2O_2 to form $\cdot O_2^{-}$ according to eqn (8)–(10). This species is also important in the degradation of organic pollutants.

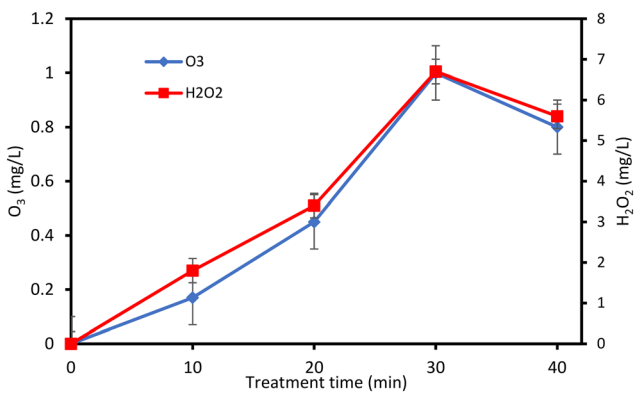

Fig. 3 Variation in the concentration of O_3 and H_2O_2 during CBZ degradation.

3.2. Investigation of key operating parameters in CBZ degradation

3.2.1. Effect of initial concentration of CBZ. The effect of the initial concentration of CBZ on its degradation efficiency using a DBD plasma system was investigated at a voltage of 6 kV, frequency of 20 kHz, and water flow rate of 500 mL min^{-1}. The results presented in Fig. 4 show that the degradation efficiency of CBZ decreased from 92% to 39% with an increase in its initial concentration from 10 to 30 mg L^{-1}. The decline in degradation efficiency is attributed to the fact that the DBD plasma generates reactive species at a rate determined by the input power and voltage. Therefore, at a constant applied voltage, the plasma discharge generates a fixed concentration of these species. On the other hand, the initial concentration of CBZ directly correlates with the number of its molecules in the solution; hence, a higher concentration of CBZ molecules relative to the number of reactive species results in lower degradation efficiency, and *vice versa*. Thus, the initial concentration of the pollutant significantly influences degradation efficiency under constant power conditions.

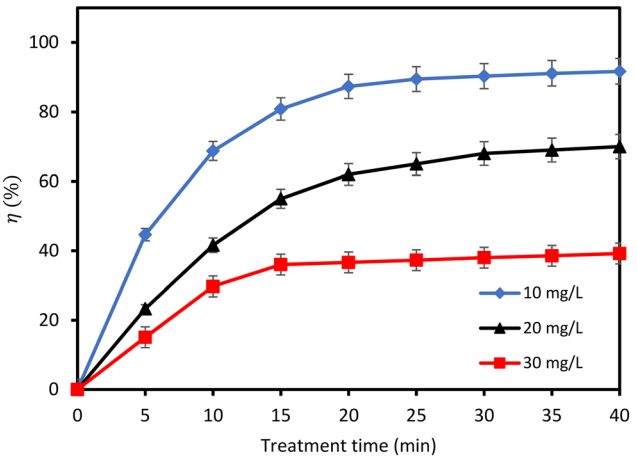

Fig. 4 Effect of CBZ initial concentration on the degradation efficiency (experimental conditions: voltage 6 kV; frequency 20 kHz).

3.2.2. Effect of applied voltage. The generation of reactive species in a DBD plasma is a defining step during the degradation of organic pollutants. An important factor that influences the production of these species is the applied voltage. To establish the impact of applied voltage on the degradation efficiency of CBZ, the DBD plasma experiments were conducted at different voltage conditions: 4, 5, and 6 kV. The results according to Fig. 5(a) clearly indicated that the degradation efficiency of CBZ improved with increasing voltage during the DBD plasma treatment. Previous literature has attributed the increase in degradation efficiency with increasing voltage to the spike in the concentration of active species in the solution.[41–43] This was confirmed in this study as seen in Fig. 5(b). An investigation of the production of H_2O_2 and O_3 showed that an increase in the applied voltage increased the concentration of both species measured in the aqueous solution.

3.2.3. Effect of solution conductivity. The conductivity of a solution has the potential to affect both the electric field intensity and ultraviolet radiation intensity of a typical NTP reactor.[44] However, this also depends on the type of reactor and the position of the discharge relative to the solution being treated.[45] In this work, the conductivity of the solution was adjusted with KCl. Fig. 6 shows the influence of solution conductivity on the degradation efficiency of CBZ. Generally, an increase in the conductivity of the solution reduced the degradation efficiency with treatment time. A notable drop in the degradation efficiency from 41% to 5% was observed as the conductivity increased from 60 μS cm^{-1} to 160 μS cm^{-1}. This is because as the conductivity increased, the spark discharge transitioned into complete corona discharges (160 μS cm^{-1}), making degradation almost impossible. This phenomenon aligns with the observations made by Yang *et al.*,[46] where the impact of conductivity was said to be due to the contact the discharge has with the aqueous solution. Given that the optimal degradation efficiency for CBZ was achieved at 5 μS cm^{-1}, which was obtained without adding KCl, other experiments were therefore conducted without conductivity adjustment.

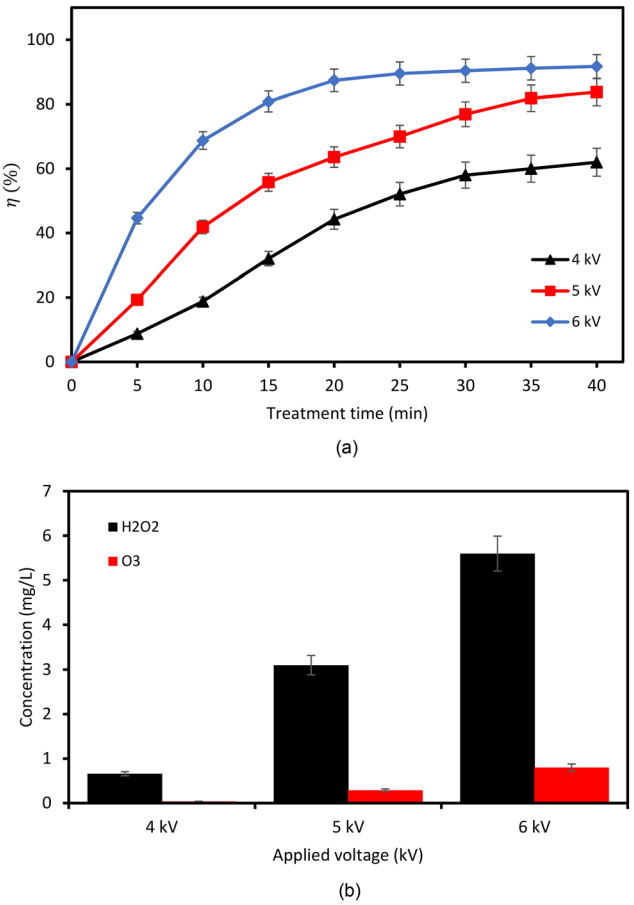

Fig. 5 (a) Applied voltage *vs.* degradation efficiency of CBZ. (b) Applied voltage *vs.* concentration of H_2O_2 and O_3 (experimental conditions: CBZ initial concentration 10 mg L^{-1}; frequency 20 kHz).

3.2.4. Effect of pH variation. Fig. 7 demonstrates how various initial pH values affect the degradation of CBZ using the DBD plasma reactor set at an applied voltage of 6 kV, frequency of 20 kHz, and initial concentration of 10 mg L^{-1}. The pH of the solution was adjusted using NaOH and

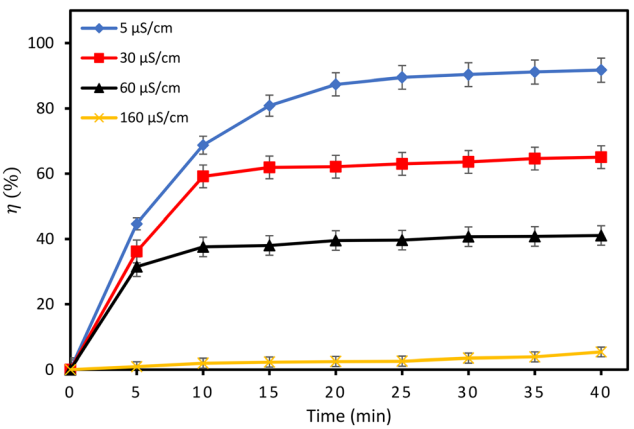

Fig. 6 Effect of solution conductivity on the degradation efficiency of CBZ (experimental conditions: CBZ initial concentration 10 mg L^{-1}; voltage 6 kV; frequency 20 kHz).

H_2SO_4 before plasma treatment. The results indicated an increase in degradation efficiency as the solution's pH shifted towards alkaline. Conversely, an acidic medium proved less effective for CBZ removal. The degradation efficiency increased to 92% as the pH rose from 3 to 5.7 (pH of the synthetic solution), then continued to >99% efficiency with further pH increase.

During water treatment, the production of active species and other radicals influenced both the pH and conductivity of the aqueous solution. The variations of these parameters at optimum conditions of initial concentration of CBZ, applied voltage, and conductivity are shown in Fig. 8. As observed, the pH of the solution decreased sharply from 5.7 to 4.97 in the first 5 min of treatment, followed by a small steady decline over the next minutes. In contrast, the conductivity of the solution maintained a consistent rise over the 40 min treatment time from 5 μS cm^{-1} to 233 μS cm^{-1}. Consequently, the degradation of CBZ with an atmospheric air DBD plasma led to an increase in the conductivity but a reduction in the pH of the aqueous medium. The reduction in pH can be attributed to the production of NO_2^- and NO_3^- during the plasma treatment with air. These active nitrogen species are products of the dissolution of nitrogen oxides (NO_x) produced by the reaction between N_2 and O_2. They also lead to the formation of acidic HNO_2 and HNO_3 in the solution.[47] The formation of nitrous acids was also confirmed by Aggelopoulos *et al.*[48] and Roglić *et al.*,[49] amongst others. However, it should be noted that when using gases other than air or nitrogen, NO_x compounds may not be formed, and thus the pH may remain affected, as confirmed by Meropoulis *et al.*[50]

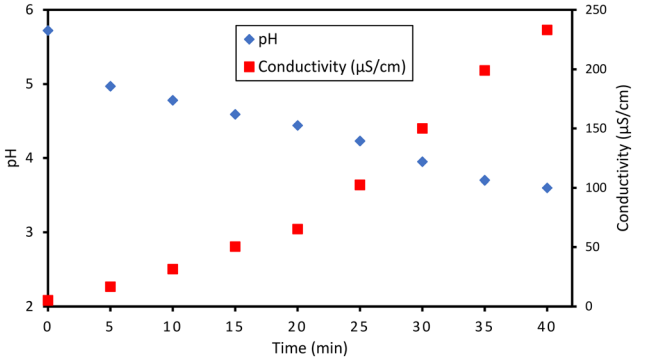

Fig. 8 pH and conductivity trends for the control solution *versus* treatment time (experimental conditions: CBZ initial concentration 10 mg L^{-1}, voltage 6 kV; frequency 20 kHz).

3.3. Investigating the effect of radical scavengers

3.3.1. Role of ·OH. In this study, the role of ·OH on the degradation of CBZ was investigated by adding IPA into the aqueous solution to quench the reactive species. IPA was selected due to its ability to effectively react with ·OH with a reaction rate of 1.9 × 10^9 mol L^{-1} s^{-1}; thus, possible reactions with the active species become inhibited.[51] According to Fig. 9, the addition of IPA significantly reduced the degradation of CBZ. This inhibition effect was more obvious as the concentration of the radical scavenger increased. About 92% degradation of CBZ was achieved without IPA after 40 min plasma treatment, and this was reduced to 63% and 50% with the addition of 3 and 6 mmol L^{-1} IPA, respectively. Also, upon increasing the concentration of IPA from 3 mmol to 6 mmol L^{-1}, the rate of the reaction reduced by 33%. Similarly, the reaction rate constant was reduced by a third as the concentration of IPA increased from 3 mmol L^{-1} to 6 mmol L^{-1}. These observations confirm that ·OH played a decisive role in the degradation of CBZ.

3.3.2. Role of $\cdot O_2^-$. The formation of $\cdot O_2^-$ in the solution can be linked to the chain reaction occurring between O_2 and H_2O_2 as described earlier. This species is also an important facilitator for the degradation of organic pollutants with a DBD process.[52] The impact of $\cdot O_2^-$ was examined in the presence of its scavenger, which is commonly BZQ with a reaction rate of 2 × 10^9 mol L^{-1} s^{-1}.[53] As observed in Fig. 10,

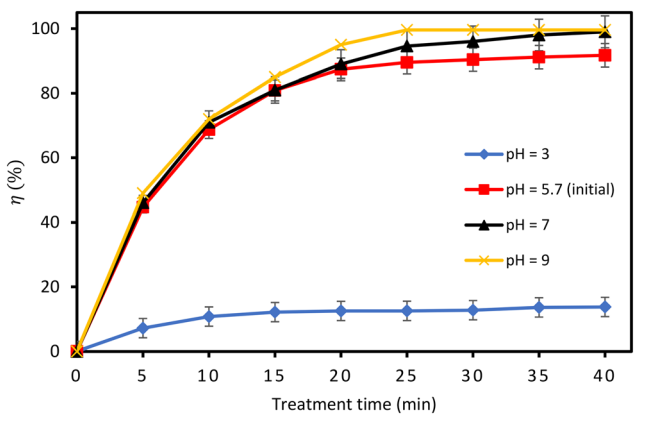

Fig. 7 Degradation efficiency at different initial pH values (experimental conditions: CBZ initial concentration 10 mg L^{-1}, voltage 6 kV; frequency 20 kHz).

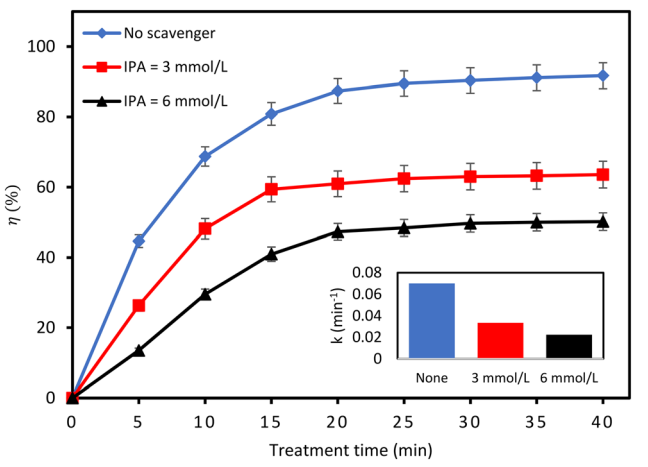

Fig. 9 Influence of isopropanol on the degradation efficiency of CBZ (experimental conditions: CBZ initial concentration 10 mg L^{-1}; voltage 6 kV; frequency 20 kHz).

the degradation efficiency for CBZ was significantly inhibited by the addition of BZQ and the rate of inhibition increased with the concentration of the radical scavenger in the solution. When the concentration of BZQ was 0.5 mmol L^{-1}, the degradation efficiency observed for CBZ was reduced from 92% to 57%, reducing the reaction rate by more than half in 40 min. A further increase in BZQ concentration to 1 mmol L^{-1} reduced the degradation efficiency further to 41% and the rate of the reaction was reduced by 38%. Similarly, the rate constant was reduced by a quarter compared with the value obtained without BZQ at this concentration. These results therefore confirm that the $\cdot O_2^-$ generated in the DBD plasma must have played a role in the degradation of CBZ.

3.3.3. Role of O_3. Ozone (O_3) gas is one of the long-lived reactive species generated by NTP reactors. Several studies have reported its potency in the oxidation of organic compounds.[54–57] In this study, UA was used to quench the possible effect of O_3 in the system in order to investigate its possible role in the degradation of CBZ. UA reacts with ozone at a rate of 1.4×10^6 mol L^{-1} s^{-1}.[51,58] Upon the addition of UA, the degradation efficiency of CBZ significantly dropped to about 18% from 92% (without UA) over the 40 min treatment time, as indicated in Fig. 11. Increasing the concentration of UA in the solution had very minimal effect on the degradation efficiency of CBZ. Also, the rate of the reaction in the presence of UA reduced by 92% compared to the control solution, while an increase in UA concentration from 0.5 to 1 mmol L^{-1} had little effect on its kinetics. Thus, the degradation of CBZ was significantly inhibited by UA regardless of its concentration. These results demonstrate that CBZ is strongly oxidized by O_3.

3.3.4. Role of H_2O_2. The role of H_2O_2 generated in the DBD plasma system was also investigated. While this species may be unstable in solution, it also contributes to the overall degradation of organic pollutants due to its strong oxidation potential ($E°$ = 1.78 V) and by its decomposition to OH radicals (Zeghioud *et al.*, 2020 (ref. 39)). A previous study has reported that SP can be used to abstract H_2O_2 species in

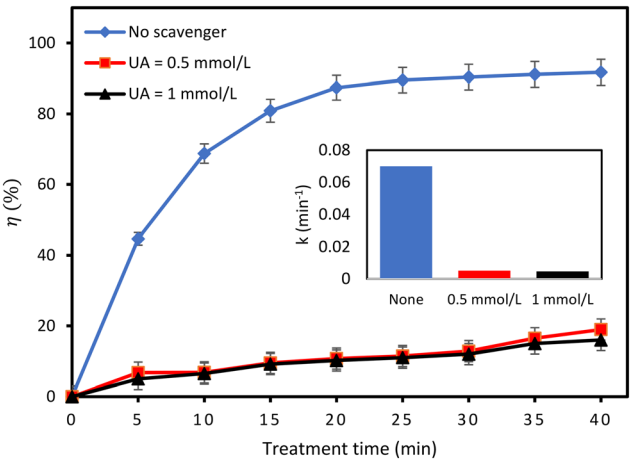

Fig. 11 Influence of uric acid on the degradation efficiency of CBZ (experimental conditions: CBZ initial concentration 10 mg L^{-1}; voltage 6 kV; frequency 20 kHz).

solution with a reaction rate of 2.4 mol L^{-1} s^{-1}.[59] According to Fig. 12, the addition of 0.5 mmol L^{-1} SP to the aqueous solution reduced the degradation efficiency of CBZ from 92% to 29% over 40 min treatment time. This further reduced to 7.5% when the concentration of SP in the solution was doubled. Similarly, the rate of the reaction reduced by 83% with 0.5 mmol L^{-1} initial concentration of SP and by 78% when SP concentration was doubled. Also, the rate constant dropped by 1/28th as the concentration of SP in the solution increased to 1 mmol L^{-1}. These results highlight the importance of H_2O_2 in the degradation of CBZ using the DBD plasma system.

3.4. Effect of different water matrices on CBZ degradation

In addition to the synthetic solution, the degradation of CBZ was also studied in two other water matrices as shown in

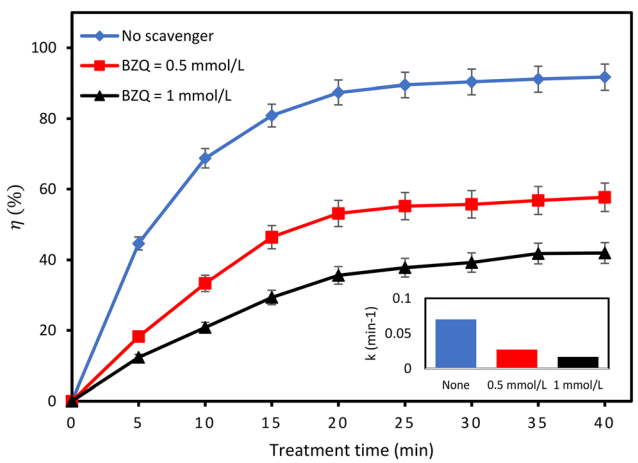

Fig. 10 Influence of *p*-benzoquinone on the degradation efficiency of CBZ (experimental conditions: CBZ initial concentration 10 mg L^{-1}; voltage 6 kV; frequency 20 kHz).

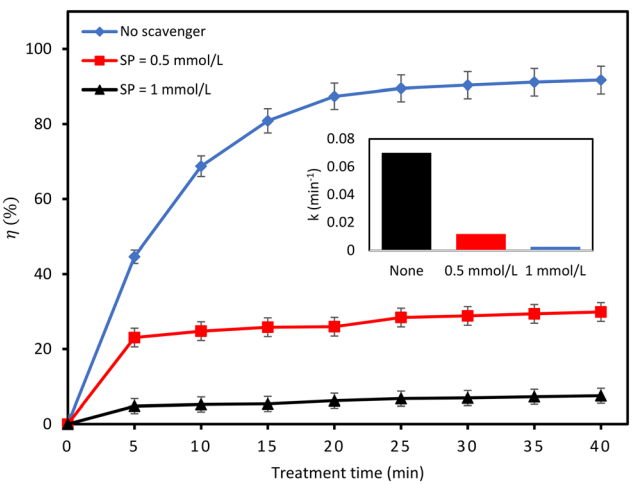

Fig. 12 Influence of sodium pyruvate on the degradation efficiency of CBZ (experimental conditions: CBZ initial concentration 10 mg L^{-1}; voltage 6 kV; frequency 20 kHz).

Fig. 13. The chemical compositions of the different water matrices, namely deionized water (DI), tap water (TW) and final wastewater effluent (FW), are summarized in Table 2. According to Fig. 13(a), the degradation efficiency observed in TW and FW was 33% and 13%, respectively, compared to 92% in DI. Similarly, the rate constant of 0.08 min^{-1} observed in DI decreased to 0.01 min^{-1} in TW and 0.004 min^{-1} in FW, as shown in Fig. 13(b). These observations can be attributed to the different matrix compositions. The presence of inorganic ions such as chloride (Cl^-), hydrogen carbonate (HCO_3^-), nitrate (NO_3^-), and sulphate (SO_4^{2-}) may have a negative impact on the degradation of CBZ with DBD plasma, leading to a significant reduction in the degradation efficiency. Cl^- and HCO_3^- are particularly impactful due to their concentrations in the TW and FW matrices and their ability to react with ·OH, a significant species facilitating the removal of CBZ with the DBD reactor. Nitrate, as noted by Palma *et al.*,[60] effectively scavenges aqueous electrons.

Table 3 shows minimal changes in the pH and conductivity for TW and FW compared to DI during plasma treatment. In TW, the pH varied between 7.3 and 7.5, and in FW, it ranged from 7.3 to 8.3. During the treatment, the conductivity of TW slightly increased from 270 to 290 μS cm^{-1}, while in FW, it rose from 544 to 617 μS cm^{-1}. Contrary to these observations, the conductivity of the DI matrix increased significantly as previously observed with DBD plasma.[47,61] Generally, when using solutions like DI which have high purity, the pH decreases while the conductivity rises significantly during plasma treatment. Whereas inorganic ions like HCO_3^- act as a pH buffer in TW and FW thus ensuring that the pH remains fairly constant during plasma treatment despite the formation of nitrogen compounds.

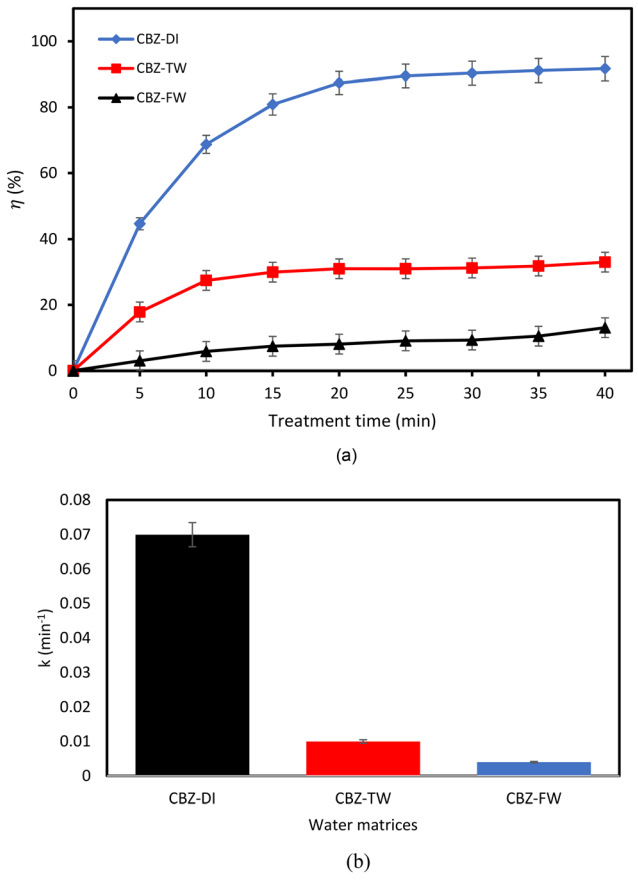

Fig. 13 (a) Effect of water matrices on degradation efficiency of CBZ. (b) Effect of water matrices on reaction rate for CBZ degradation (experimental conditions: CBZ initial concentration 10 mg L^{-1}; voltage 6 kV; frequency 20 kHz).

3.5. Comparison of the removal of CBZ in DBD plasma and UV-based systems

3.5.1. Degradation efficiency and kinetics. The most frequently researched AOPs for the degradation of CBZ are photochemical oxidation techniques like UV/H_2O_2, photo-Fenton and photocatalysis. However, it is often challenging to compare the reported results from the literature where different methods have been used due to variations in experimental conditions such as initial concentration, volume of solution, solvent matrix, input power, amongst others. To facilitate a more direct comparison, this study employed a UV-based system to treat a similar concentration of CBZ (10 mg L^{-1}) in the same water matrix (deionized water). Comparing the performance of the atmospheric air DBD plasma in this study with that of UV-based technology, which has reached full-scale commercialization, offers a reliable basis to assess the efficacy of the DBD plasma technology. The choice of UV-based technology was influenced by its documented success in removing organic pollutants like CBZ.[14,62] Both the UV and plasma experiments treated 500 mL containing 10 mg L^{-1} CBZ.

As depicted in Fig. 14(a) and (b), a UV-only condition achieved a CBZ degradation of 6.5% and a rate constant of 0.0021 min^{-1}, in 40 min. This result is consistent with previous findings.[63–65] The degradation resistance of CBZ under a UV-only condition can be attributed to the presence of an amide group ($RCONH_2$) in the molecule.[64] Meanwhile, the addition of Fe^{2+} slightly increased the degradation efficiency to 17.7% and 0.0051 min^{-1} under the same condition. UV/H_2O_2 is one of the most studied oxidation systems that has also been commercially deployed for the removal of organic pollutants. In this process, UV irradiates H_2O_2 to form ·OH resulting in an increased degradation efficiency to about 90.3% in 40 min. Also, the addition of Fe^{2+} to the UV/H_2O_2 setup slightly increased the degradation efficiency and rate of the reaction by a possible Fenton reaction occurring in the solution.[52,66] An improvement in a UV-based reaction with the addition of H_2O_2 and Fe^{2+} was also confirmed in a study by Ali *et al.*[14] Meanwhile, the DBD plasma system yielded a 98% degradation efficiency for CBZ at the operating conditions considered and a rate constant of 0.13 min^{-1}.

3.5.2. Energy efficiency. From an industrial-application perspective, another important factor that can be used for

Table 3 Variation of pH and conductivity during the degradation of CBZ in tap water and final wastewater effluent

Parameters	Deionized water	Tap water	Final wastewater effluent
Initial pH	5.7	7.5	7.3
Final pH	3.6	7.3	8.3
Initial conductivity (μS cm^{-1})	5	270	544
Final conductivity (μS cm^{-1})	233	290	617

comparing water treatment methods in addition to degradation efficiency is the energy efficiency, which also directly affects the energy cost of treatment. The electrical energy per order (E_{EO}) is a valuable figure-of-merit for assessing energy efficiency, as introduced by Bolton *et al.* (2001).[67] E_{EO} measures the electrical energy (kW h) required to degrade a targeted pollutant by one order of magnitude per cubic meter of water. This method has been reported to be suitable for conditions in which the concentration of the pollutant is low, and for pseudo-first-order reactions. E_{EO} was calculated using eqn (11):[67]

$$E_{EO} = \frac{P \cdot t \cdot 1000}{V \cdot 60 \cdot \log\left(\frac{C_i}{C_f}\right)} \quad (11)$$

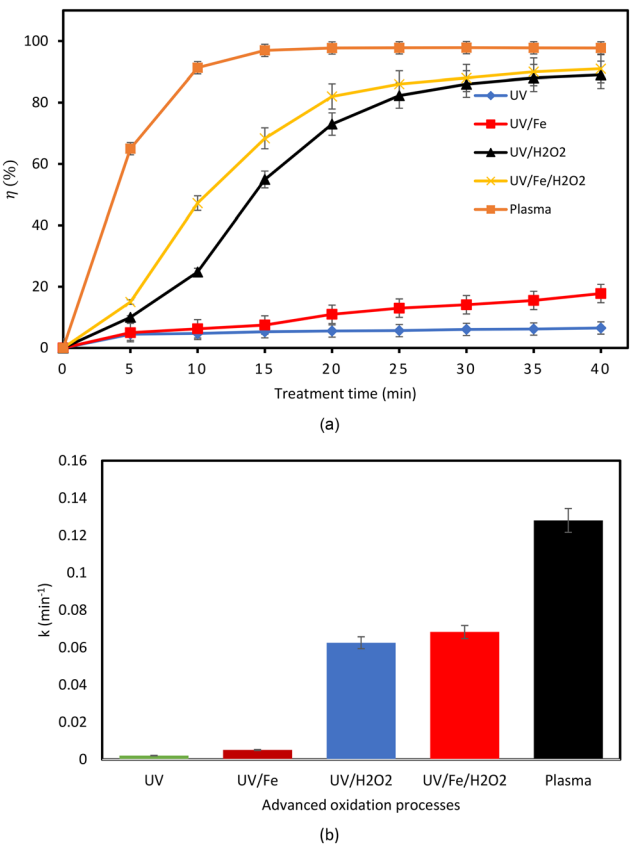

Fig. 14 (a) Comparison of the different AOPs in terms of degradation efficiency. (b) Comparison of the different AOPs in terms of reaction kinetics (experimental conditions: volume of solution = 500 mL; initial CBZ concentration = 10 mg L^{-1}).

where P is the power introduced into the system (kW), t is the treatment time (min), V is the volume of the solution (L), C_i is the initial concentration of CBZ and C_f is the final concentration of CBZ after 40 min treatment time. With the introduction of the first-order rate equation, eqn (12) can be derived from eqn (11):

$$E_{EO} = \frac{38.4P}{V \cdot k} \quad (12)$$

It should be noted that the power (P) mentioned in eqn (11) and (12) reflects the total power consumption of the AOPs considered. The vast majority of literature dealing with energy efficiency only specifies the power used in generating the chemical species, neglecting the energy consumed by the instrument itself and other possible energy losses. This can make direct comparisons between different technologies somewhat skewed. In this study, the power consumed for the AOPs was measured with an AC power meter (Schweitzer Engineering Laboratories, USA). The plasma and UV systems drew 125 W and 250 W from the grid, respectively.

The energy cost of treatment, expressed in USD per cubic meter, was estimated by multiplying the energy efficiency (E_{EO}) with the electricity price for the region in which the study was conducted (Tshwane, South Africa). Table 5 presents the energy efficiency and corresponding energy cost of treatment for the various AOPs examined in this study. The pseudo-first-order reaction rate constants needed to estimate E_{EO} were taken from the kinetic data reported in Table 4. Furthermore, the average electricity tariff in Tshwane municipality for the category >650 kW h is approximately ZAR 3.32/kW h (equivalent to 0.17 USD per kW h according to Oanda rates) (City of Tshwane, 2023). From the data in Table 5, the energy efficiency spans a wide range of 75.24–9142.86 kW h m^{-3}, covering over two orders of magnitude. The energy efficiencies for the UV systems (281.11–9142.86 kW h m^{-3}) were significantly higher than

Table 4 Comparison of the degradation efficiency and kinetics for the different AOP setups used in this study (solution volume = 500 mL, initial pollutant concentration = 10 mg L^{-1})

Technology	Fe [mol L^{-1}]	H_2O_2 [mol L^{-1}]	Kinetics (min^{-1})	CBZ solution (L)	η (%)
UV	0	0	0.0021	0.5	6.5
UV/Fe	72	0	0.0051	0.5	17.8
UV/H_2O_2	0	250	0.0630	0.5	89
UV/Fe/H_2O_2	72	250	0.0683	0.5	91
Plasma	0	0	0.1281	0.5	98

Table 5 Comparison of the energy efficiency and associated costs of treatment for the AOPs considered in this work

AOP	E_{EO} (kW h m^{-3})	Energy cost of treatment (USD per m^3)
UV	9142.86	1554
UV/Fe	3764.71	640
UV/H_2O_2	306.70	52
UV/Fe/H_2O_2	281.11	48
Plasma	75.24	13

that of the plasma system (75.24 kW h m^{-3}). Meanwhile, a photolysis system without any additive is observed to be the most inefficient technology for treating CBZ. From a cost of treatment perspective, the UV systems were at least three times more costly than the plasma system. Again, it should be noted that the cost described in this study is not wholistic as it does not take into consideration the capital expense of the technology and operational and maintenance costs. It only reflects the performance of the technology from an energy cost perspective.

4. Conclusions

This study utilized an atmospheric air DBD plasma for the treatment of CBZ-polluted water, exploring the influence of operating parameters like initial concentration, applied voltage, pH, and conductivity of the solution on the DBD performance in terms of CBZ degradation efficiency. It was observed that a higher initial concentration of CBZ led to a reduced active species-to-CBZ molecule ratio, decreasing the degradation efficiency. Meanwhile, higher applied voltage favoured the production of reactive species, which enhanced the degradation efficiency. Optimal degradation of the pollutant occurred at neutral pH to more alkaline conditions, whereas an increase in the conductivity of the solution changed the discharge scheme from spark to corona, thus reducing the degradation efficiency. At operating conditions of 6 kV voltage, 20 kHz frequency, 10 mg L^{-1} initial CBZ concentration and 5 μS cm^{-1} conductivity, approximately 92% CBZ degradation was achieved.

Also, this study delved into the degradation mechanism for CBZ with the atmospheric DBD plasma, by examining the concentration and the quenching effect of radical scavengers at different concentrations. The results showed that O_3 played the most significant role in CBZ degradation followed by ·OH, H_2O_2 and $\cdot O_2^-$. The reactive nitrogen species played a role in the acidification of the solution during plasma treatment. To get closer to real conditions, the DBD experiments were also conducted in tap water and in final wastewater effluent from a municipality. Significant inhibitions were observed in the final wastewater effluent matrix, followed by tap water as compared to deionized water during the 40 min treatment. This was due to the presence of naturally occurring organic and inorganic molecules in the water matrices. The DBD system was also compared with commercialized UV systems in terms of degradation efficiency and associated energy cost of treatment. At a similar solution volume (500 mL) and initial concentration of CBZ, the degradation efficiencies obtained are 6.5%, 17.8%, 89%, 91%, and 98%, for UV-only, UV/Fe, UV/H_2O_2, UV/Fe/H_2O_2 and the DBD plasma, respectively. Also, the plasma system had the highest energy efficiency (75.24 kW h m^{-3}) and the least required energy cost of treatment (13 USD per m^3) compared to the UV systems considered.

Data availability

All the new data generated experimentally for this article for analysis are presented either in tables or in figures within the paper. Additional data sharing is not applicable to this article.

Conflicts of interest

The authors hereby declare that they have no competing interests that could have appeared to influence the work reported in this paper.

Acknowledgements

This research was supported by the Government of the United Kingdom through The Royal Society FLAIR award [FLR \R1\201683]. We would also like to acknowledge all final-year undergraduate students who assisted in the laboratory work: Andrea D'sa, Klu Enyonam and Calvin.

References

1 C. G. Daughton and T. A. Ternes, Pharmaceuticals and personal care products in the environment: agents of subtle change?, *Environ. Health Perspect.*, 1999, **107**(suppl 6), 907–938, DOI: **10.1289/ehp.99107s6907**.
2 T. A. Ternes, Occurrence of drugs in German sewage treatment plants and rivers, Dedicated to Professor Dr. Klaus Haberer on the occasion of his 70th birthday, *Water Res.*, 1998, **32**(11), 3245–3260, DOI: **10.1016/S0043-1354(98)00099-2**.
3 T. Ternes, A. Joss and J. Oehlmann, Occurrence, fate, removal and assessment of emerging contaminants in water in the water cycle (from wastewater to drinking water), *Water Res.*, 2015, **72**, 1–2, DOI: **10.1016/j.watres.2015.02.055**.
4 R. Gurke, M. Rößler and C. Marx, *et al.*, Occurrence and removal of frequently prescribed pharmaceuticals and corresponding metabolites in wastewater of a sewage treatment plant, *Sci. Total Environ.*, 2015, **532**, 762–770, DOI: **10.1016/j.scitotenv.2015.06.067**.
5 P. K. Mutiyar, S. K. Gupta and A. K. Mittal, Fate of pharmaceutical active compounds (PhACs) from River Yamuna, India: An ecotoxicological risk assessment approach, *Ecotoxicol. Environ. Saf.*, 2018, **150**, 297–304, DOI: **10.1016/j.ecoenv.2017.12.041**.
6 W. Zhao, G. Yu, L. Blaney and B. Wang, Development of emission factors to estimate discharge of typical pharmaceuticals and personal care products from

wastewater treatment plants, *Sci. Total Environ.*, 2021, **769**, 144556, DOI: **10.1016/j.scitotenv.2020.144556**.

7 C. F. Couto, L. C. Lange and M. C. S. Amaral, Occurrence, fate and removal of pharmaceutically active compounds (PhACs) in water and wastewater treatment plants—A review, *J. Water Process Eng.*, 2019, **32**, 100927, DOI: **10.1016/j.jwpe.2019.100927**.

8 F. I. Hai, S. Yang, M. B. Asif, V. Sencadas, S. Shawkat, M. Sanderson-Smith, J. Gorman, Z.-Q. Xu and K. Yamamoto, Carbamazepine as a Possible Anthropogenic Marker in Water: Occurrences, Toxicological Effects, Regulations and Removal by Wastewater Treatment Technologies, *Water*, 2018, **10**(2), 1–32, DOI: **10.3390/w10020107**.

9 A. C. Kondor, G. Jakab, A. Vancsik, T. Filep, J. Szeberényi, L. Szabó, G. Maász, A. Ferincz, P. Dobosy and Z. Szalai, Occurrence of pharmaceuticals in the Danube and drinking water wells: Efficiency of riverbank filtration, *Environ. Pollut.*, 2020, **265**, 114893, DOI: **10.1016/j.envpol.2020.114893**.

10 N. H. Tran and K. Y.-H. Gin, Occurrence and removal of pharmaceuticals, hormones, personal care products, and endocrine disrupters in a full-scale water reclamation plant, *Sci. Total Environ.*, 2017, **599–600**, 1503–1516, DOI: **10.1016/j.scitotenv.2017.05.097**.

11 É. Hansen, P. Monteiro de Aquim and M. Gutterres, Current technologies for post-tanning wastewater treatment: A review, *J. Environ. Manage.*, 2021, **294**, 113003, DOI: **10.1016/j.jenvman.2021.113003**.

12 A. C. Sophia and E. C. Lima, Removal of emerging contaminants from the environment by adsorption, *Ecotoxicol. Environ. Saf.*, 2018, **150**, 1–17, DOI: **10.1016/j.ecoenv.2017.12.026**.

13 L. Barillas, Design of a Prototype of Water Purification by Plasma Technology as the Foundation for an Industrial Wastewater Plant, *J. Phys.: Conf. Ser.*, 2015, **591**, 012057, DOI: **10.1088/1742-6596/591/1/012057**.

14 F. Ali, J. A. Khan, N. S. Shah, M. Sayed and H. M. Khan, Carbamazepine degradation by UV and UV-assisted AOPs: Kinetics, mechanism and toxicity investigations, *Process Saf. Environ. Prot.*, 2018, **117**, 307–314, DOI: **10.1016/j.psep.2018.05.004**.

15 X. Zou, X. Li, C. Chen, X. Zhu, X. Huang, Y. Wu, Z. Pi, Z. Chen, Z. Tao, D. Wang and Q. Yang, Degradation performance of carbamazepine by ferrous-activated sodium hypochlorite: Mechanism and impacts on the soil system, *Chem. Eng. J.*, 2020, **389**, 123451, DOI: **10.1016/j.cej.2019.123451**.

16 S. Wang and N. Zhou, Removal of carbamazepine from aqueous solution using sono-activated persulfate process, *Ultrason. Sonochem.*, 2016, **29**, 156–162, DOI: **10.1016/j.ultsonch.2015.09.008**.

17 H. Guo, X. Zhou, Y. Zhang, Q. Yao, Y. Qian, H. Chu and J. Chen, Carbamazepine degradation by heterogeneous activation of peroxymonosulfate with lanthanum cobaltite perovskite: Performance, mechanism and toxicity, *J. Environ. Sci.*, 2020, **91**, 10–21, DOI: **10.1016/j.jes.2020.01.003**.

18 K. Roy and V. S. Moholkar, Mechanistic analysis of carbamazepine degradation in hybrid advanced oxidation process of hydrodynamic cavitation/UV/persulfate in the presence of ZnO/$ZnFe_2O_4$, *Sep. Purif. Technol.*, 2021, **270**, 118764, DOI: **10.1016/j.seppur.2021.118764**.

19 Y. Ding, G. Zhang, X. Wang, L. Zhu and H. Tang, Chemical and photocatalytic oxidative degradation of carbamazepine by using metastable Bi^{3+} self-doped $NaBiO_3$ nanosheets as a bifunctional material, *Appl. Catal., B*, 2017, **202**, 528–538, DOI: **10.1016/j.apcatb.2016.09.054**.

20 S. Dudziak, A. Fiszka Borzyszkowska and A. Zielińska-Jurek, Photocatalytic degradation and pollutant-oriented structure-activity analysis of carbamazepine, ibuprofen and acetaminophen over faceted TiO_2, *J. Environ. Chem. Eng.*, 2023, **11**(2), 109553, DOI: **10.1016/j.jece.2023.109553**.

21 L. Bo, K. He, N. Tan, B. Gao, Q. Feng, J. Liu and L. Wang, Photocatalytic oxidation of trace carbamazepine in aqueous solution by visible-light-driven $Znln_2S_4$: Performance and mechanism, *J. Environ. Manage.*, 2017, **190**, 259–265, DOI: **10.1016/j.jenvman.2016.12.050**.

22 R. Meribout, Y. Zuo, A. A. Khodja, A. Piram, S. Lebarillier, J. Cheng, C. Wang and P. Wong-Wah-Chung, Photocatalytic degradation of antiepileptic drug carbamazepine with bismuth oxychlorides (BiOCl and BiOCl/AgCl composite) in water: Efficiency evaluation and elucidation degradation pathways, *J. Photochem. Photobiol., A*, 2016, **328**, 105–113, DOI: **10.1016/j.jphotochem.2016.04.024**.

23 A. Asghar, M. Hammad, K. Kerpen, F. Niemann, A. K. Al-Kamal, D. Segets, H. Wiggers and T. C. Schmidt, Ozonation of carbamazepine in the presence of sulfur-dopped graphene: Effect of process parameters and formation of main transformation products, *Sci. Total Environ.*, 2023, **864**, 161079, DOI: **10.1016/j.scitotenv.2022.161079**.

24 B. Yang, J. Deng, G. Yu, S. Deng, J. Li, C. Zhu, Q. Zhuo, H. Duan and T. Guo, Effective degradation of carbamazepine using a novel electro-peroxone process involving simultaneous electrochemical generation of ozone and hydrogen peroxide, *Electrochem. Commun.*, 2018, **86**, 26–29, DOI: **10.1016/j.elecom.2017.11.003**.

25 Y. Liu, S. Mei, D. Iya-Sou, S. Cavadias and S. Ognier, Carbamazepine removal from water by dielectric barrier discharge: Comparison of ex situ and in situ discharge on water, *Chem. Eng. Process.: Process Intesif.*, 2012, **56**, 10–18, DOI: **10.1016/j.cep.2012.03.003**.

26 H. Krause, B. Schweiger, J. Schuhmacher, S. Scholl and U. Steinfeld, Degradation of the endocrine disrupting chemicals (EDCs) carbamazepine, clofibric acid, and iopromide by corona discharge over water, *Chemosphere*, 2009, **75**(2), 163–168, DOI: **10.1016/j.chemosphere.2008.12.020**.

27 E. Gwanzura, D. Ramjugernath and S. A. Iwarere, Removal efficiency and energy consumption optimization for carbamazepine degradation in wastewater by electrohydraulic discharge, *Water Environ. Res.*, 2023, **95**(8), e10915, DOI: **10.1002/wer.10915**.

28 M. P. Rayaroth, O. Aubry, H. Rabat, E. Marilleau, Y. Gru, D. Hong and P. Brault, Degradation and transformation of carbamazepine in aqueous medium under non-thermal

plasma oxidation process, *Chemosphere*, 2024, **352**, 141449, DOI: **10.1016/j.chemosphere.2024.141449**.

29 J. Yu, W. Yan, B. Zhu, Z. Xu, S. Hu, W. Xi, Y. Lan, W. Han and C. Cheng, Degradation of carbamazepine by high-voltage direct current gas–liquid plasma with the addition of H_2O_2 and Fe^{2+}, *Environ. Sci. Pollut. Res.*, 2022, **29**(51), 77771–77787, DOI: **10.1007/s11356-022-21250-6**.

30 K. Ahlawat, R. Jangra and R. Prakash, Degradation of carbamazepine and sulfamethoxazole in water by dielectric barrier discharge plasma coupled with a far UV-C (222 nm) system, *Environ. Sci.: Water Res. Technol.*, 2024, **10**(12), 3122–3136, DOI: **10.1039/D4EW00564C**.

31 S. Kooshki, P. Pareek, R. Mentheour, M. Janda and Z. Machala, Efficient treatment of bio-contaminated wastewater using plasma technology for its reuse in sustainable agriculture, *Environ. Technol. Innovation*, 2023, **32**, 103287, DOI: **10.1016/j.eti.2023.103287**.

32 V. V. Kovačević, B. P. Dojčinović, M. Jović, G. M. Roglić, B. M. Obradović and M. M. Kuraica, Measurement of reactive species generated by dielectric barrier discharge in direct contact with water in different atmospheres, *J. Phys. D: Appl. Phys.*, 2017, **50**(15), 155205, DOI: **10.1088/1361-6463/aa5fde**.

33 B. N. Magaela, K. S. Ndlovu, C. S. Tshangana, A. A. Muleja, B. B. Mamba, T. Nyokong and M. Managa, Photodegradation of ibuprofen using 5-10-15-20-tetrakis(4-bromophenyl) porphyrin conjugated to graphene quantum dots, *Opt. Mater.*, 2022, **134**, 113147, DOI: **10.1016/j.optmat.2022.113147**.

34 S. Zwane, D. S. Dlamini, B. B. Mamba and A. T. Kuvarega, Evaluation of the photodegradation of pharmaceuticals and dyes in water using a highly visible light-active graphitic carbon nitride modified with tungsten oxide, *Inorg. Chem. Commun.*, 2023, **151**, 110637, DOI: **10.1016/j.inoche.2023.110637**.

35 M. Magureanu, F. Bilea, C. Bradu and D. Hong, A review on non-thermal plasma treatment of water contaminated with antibiotics, *J. Hazard. Mater.*, 2021, **417**, 125481, DOI: **10.1016/j.jhazmat.2021.125481**.

36 P. Lukes, B. R. Locke and J.-L. Brisset, Aqueous-Phase Chemistry of Electrical Discharge Plasma in Water and in Gas–Liquid Environments, *Plasma Chem. Catal. Gases Liq.*, 2012, 243–308.

37 B. R. Locke and K.-Y. Shih, Review of the methods to form hydrogen peroxide in electrical discharge plasma with liquid water, *Plasma Sources Sci. Technol.*, 2011, **20**(3), 034006, DOI: **10.1088/0963-0252/20/3/034006**.

38 M. J. Kirkpatrick and B. R. Locke, Hydrogen, Oxygen, and Hydrogen Peroxide Formation in Aqueous Phase Pulsed Corona Electrical Discharge, *Ind. Eng. Chem. Res.*, 2005, **44**(12), 4243–4248, DOI: **10.1021/ie048807d**.

39 H. Zeghioud, P. Nguyen-Tri, L. Khezami, A. Amrane and A. A. Assadi, Review on discharge Plasma for water treatment: mechanism, reactor geometries, active species and combined processes, *J. Water Process Eng.*, 2020, **38**, 101664, DOI: **10.1016/j.jwpe.2020.101664**.

40 C. C. Lin, F. R. Smith, N. Ichikawa, T. Baba and M. Itow, Decomposition of hydrogen peroxide in aqueous solutions at elevated temperatures, *Int. J. Chem. Kinet.*, 1991, **23**(11), 971–987, DOI: **10.1002/kin.550231103**.

41 D. Hong, H. Rabat, J. M. Bauchire and M. B. Chang, Measurement of Ozone Production in Non-thermal Plasma Actuator Using Surface Dielectric Barrier Discharge, *Plasma Chem. Plasma Process.*, 2014, **34**(4), 887–897, DOI: **10.1007/s11090-014-9527-3**.

42 S. Li, X. Wang, L. Liu, Y. Guo, Q. Mu and A. Mellouki, Enhanced degradation of perfluorooctanoic acid using dielectric barrier discharge with La/Ce-doped TiO2, *Environ. Sci. Pollut. Res.*, 2017, **24**(18), 15794–15803, DOI: **10.1007/s11356-017-9246-4**.

43 P. Manoj Kumar Reddy, B. Ramaraju and C. Subrahmanyam, Degradation of malachite green by dielectric barrier discharge plasma, *Water Sci. Technol.*, 2013, **67**(5), 1097–1104, DOI: **10.2166/wst.2013.663**.

44 B. Dong, P. Wang, Z. Li, W. Tu and Y. Tan, Degrading hazardous benzohydroxamic acid in the industrial beneficiation wastewater by dielectric barrier discharge reactor, *Sep. Purif. Technol.*, 2022, **299**, 121644, DOI: **10.1016/j.seppur.2022.121644**.

45 S. M. Allabakshi, P. S. N. S. R. Srikar, R. K. Gangwar and S. M. Maliyekkal, Feasibility of surface dielectric barrier discharge in wastewater treatment: Spectroscopic modeling, diagnostic, and dye mineralization, *Sep. Purif. Technol.*, 2022, **296**, 121344, DOI: **10.1016/j.seppur.2022.121344**.

46 B. Yang, L. Lei and M. Zhou, Effects of the Liquid Conductivity on Pulsed High-voltage Discharge Modes in Water, *Chin. Chem. Lett.*, 2004, **15**(10), 1215–1218.

47 S. Karoui, W. A. Saoud, A. Ghorbal, F. Fourcade, A. Amrane and A. A. Assadi, Intensification of non-thermal plasma for aqueous Ciprofloxacin degradation: Optimization study, mechanisms, and combined plasma with photocatalysis, *J. Water Process Eng.*, 2022, **50**, 103207, DOI: **10.1016/j.jwpe.2022.103207**.

48 C. A. Aggelopoulos, S. Meropoulis, M. Hatzisymeon, Z. G. Lada and G. Rassias, Degradation of antibiotic enrofloxacin in water by gas-liquid nsp-DBD plasma: Parametric analysis, effect of H_2O_2 and CaO_2 additives and exploration of degradation mechanisms, *Chem. Eng. J.*, 2020, **398**, 125622, DOI: **10.1016/j.cej.2020.125622**.

49 B. P. Dojčinović, G. M. Roglić, B. M. Obradović, M. M. Kuraica, M. M. Kostić, J. Nešić and D. D. Manojlović, Decolorization of reactive textile dyes using water falling film dielectric barrier discharge, *J. Hazard. Mater.*, 2011, **192**(2), 763–771, DOI: **10.1016/j.jhazmat.2011.05.086**.

50 S. Meropoulis, S. Giannoulia, S. Skandalis, G. Rassias and C. A. Aggelopoulos, Key-study on plasma-induced degradation of cephalosporins in water: Process optimization, assessment of degradation mechanisms and residual toxicity, *Sep. Purif. Technol.*, 2022, **298**, 121639, DOI: **10.1016/j.seppur.2022.121639**.

51 H. A. Aboubakr, U. Gangal, M. M. Youssef, S. M. Goyal and P. J. Bruggeman, Inactivation of virus in solution by cold atmospheric pressure plasma: identification of chemical inactivation pathways, *J. Phys. D: Appl. Phys.*, 2016, **49**(20), 204001, DOI: **10.1088/0022-3727/49/20/204001**.

52 Y. Li, Y. Yang, J. Lei, W. Liu, M. Tong and J. Liang, The degradation pathways of carbamazepine in advanced oxidation process: A mini review coupled with DFT calculation, *Sci. Total Environ.*, 2021, **779**, 146498, DOI: **10.1016/j.scitotenv.2021.146498**.

53 H. Zhang, P. Li, A. Zhang, J. Liu, P. Héroux and Y. Liu, Enhancing Interface Reactions by Introducing Microbubbles into a Plasma Treatment Process for Efficient Decomposition of PFOA, *Environ. Sci. Technol.*, 2021, **55**(23), 16067–16077, DOI: **10.1021/acs.est.1c01724**.

54 M. Gągol, A. Przyjazny and G. Boczkaj, Wastewater treatment by means of advanced oxidation processes based on cavitation – A review, *Chem. Eng. J.*, 2018, **338**, 599–627, DOI: **10.1016/j.cej.2018.01.049**.

55 K. H. Hama Aziz, H. Miessner, S. Mueller, D. Kalass, D. Moeller, I. Khorshid and M. A. M. Rashid, Degradation of pharmaceutical diclofenac and ibuprofen in aqueous solution, a direct comparison of ozonation, photocatalysis, and non-thermal plasma, *Chem. Eng. J.*, 2017, **313**, 1033–1041, DOI: **10.1016/j.cej.2016.10.137**.

56 Z. Li, Y. Wang, H. Guo, S. Pan, C. Puyang, Y. Su, W. Qiao and J. Han, Insights into water film DBD plasma driven by pulse power for ibuprofen elimination in water: performance, mechanism and degradation route, *Sep. Purif. Technol.*, 2021, **277**, 119415, DOI: **10.1016/j.seppur.2021.119415**.

57 D. Mousel, D. Bastian, J. Firk, L. Palmowski and J. Pinnekamp, Removal of pharmaceuticals from wastewater of health care facilities, *Sci. Total Environ.*, 2021, **751**, 141310, DOI: **10.1016/j.scitotenv.2020.141310**.

58 H. Guo, N. Jiang, H. Wang, K. Shang, N. Lu, J. Li and Y. Wu, Enhanced catalytic performance of graphene-TiO2 nanocomposites for synergetic degradation of fluoroquinolone antibiotic in pulsed discharge plasma system, *Appl. Catal., B*, 2019, **248**, 552–566, DOI: **10.1016/j.apcatb.2019.01.052**.

59 T. Zhang, R. Zhou, P. Wang, A. Mai-Prochnow, R. McConchie, W. Li, R. Zhou, E. W. Thompson, K. K. Ostrikov and P. J. Cullen, Degradation of cefixime antibiotic in water by atmospheric plasma bubbles: Performance, degradation pathways and toxicity evaluation, *Chem. Eng. J.*, 2021, **421**, 127730, DOI: **10.1016/j.cej.2020.127730**.

60 D. Palma, C. Richard and M. Minella, State of the art and perspectives about non-thermal plasma applications for the removal of PFAS in water, *Chem. Eng. J. Adv.*, 2022, **10**, 100253, DOI: **10.1016/j.ceja.2022.100253**.

61 E. Marotta, E. Ceriani, M. Schiorlin, C. Ceretta and C. Paradisi, Comparison of the rates of phenol advanced oxidation in deionized and tap water within a dielectric barrier discharge reactor, *Water Res.*, 2012, **46**(19), 6239–6246, DOI: **10.1016/j.watres.2012.08.022**.

62 M. Xu, J. Deng, A. Cai, C. Ye, X. Ma, Q. Li, S. Zhou and X. Li, Synergistic effects of UVC and oxidants (PS vs. Chlorine) on carbamazepine attenuation: Mechanism, pathways, DBPs yield and toxicity assessment, *Chem. Eng. J.*, 2021, **413**, 127533, DOI: **10.1016/j.cej.2020.127533**.

63 J. Deng, Y. Shao, N. Gao, S. Xia, C. Tan, S. Zhou and X. Hu, Degradation of the antiepileptic drug carbamazepine upon different UV-based advanced oxidation processes in water, *Chem. Eng. J.*, 2013, **222**, 150–158, DOI: **10.1016/j.cej.2013.02.045**.

64 I. Kim and H. Tanaka, Photodegradation characteristics of PPCPs in water with UV treatment, *Environ. Int.*, 2009, **35**(5), 793–802, DOI: **10.1016/j.envint.2009.01.003**.

65 S. Miralles-Cuevas, D. Darowna, A. Wanag, S. Mozia, S. Malato and I. Oller, Comparison of UV/H2O2, UV/S2O82−, solar/Fe(II)/H2O2 and solar/Fe(II)/S2O82− at pilot plant scale for the elimination of micro-contaminants in natural water: An economic assessment, *Chem. Eng. J.*, 2017, **310**, 514–524, DOI: **10.1016/j.cej.2016.06.121**.

66 M. A. Oturan and J.-J. Aaron, Advanced Oxidation Processes in Water/Wastewater Treatment: Principles and Applications. A Review, *Crit. Rev. Environ. Sci. Technol.*, 2014, **44**(23), 2577–2641, DOI: **10.1080/10643389.2013.829765**.

67 J. R. Bolton, K. G. Bircher, W. Tumas and C. A. Tolman, Figures-of-Merit for the Technical Development and Application of Advanced Oxidation Technologies for Both Electric and Solar-Driven Systems, *Pure Appl. Chem.*, 2001, **73**(4), 627–637, DOI: **10.1351/pac200173040627**.